Solute relaxation on the solvatochromism of *ortho*-betaine dyes. A sequential Monte Carlo/quantum mechanics study

Marcelo Zaldini Hernandes,[a] Ricardo Longo,[b] Kaline Coutinho[c] and Sylvio Canuto*[d]

[a] *Depto. de Ciências Farmacêuticas, Univ. Federal de Pernambuco, 50740-521 Recife, PE, Brazil. E-mail: zaldini@ufpe.br*
[b] *Depto. de Química Fundamental, Univ. Federal de Pernambuco, 50740-540 Recife, PE, Brazil. E-mail: longo@ufpe.br*
[c] *Universidade de Mogi das Cruzes/CIIB, CP: 411, 08701-970 Mogi das Cruzes, SP, Brazil. E-mail: kaline@umc.br*
[d] *Instituto de Física, Universidade de São Paulo, CP: 66318, 05315-970 São Paulo, SP, Brazil. E-mail: canuto@if.usp.br; Fax: +55 11 30916831; Tel: +55 11 30916980*

Molecular relaxation in solution, estimated by thermodynamic perturbation theory, is shown to be important even for a qualitative description of the solvent effects on the solvatochromic shifts of flexible betaine dyes. It is shown that the most stable conformer of the *ortho*-betaine has a dihedral angle $\varphi = 30°$ in the gas phase and $\varphi = 60°$ in aqueous solution. This relaxation alone is responsible for about 30% of the overall blue shift observed in the $n \rightarrow \pi^*$ transition of betaine in water. In addition, it was observed that the $\pi \rightarrow \pi^*$ transitions are actually red shifted in the gas phase due to internal rotation. The total solvatochromism of about 6000 cm^{-1} estimated with a Monte Carlo/quantum mechanics sequential methodology is in reasonable agreement with the experimental shift of the absorption spectra in water and in toluene.

Introduction

Conjugated organic compounds that present large changes of the dipole moment upon electronic excitation are of great interest mainly due to the strong solvatochromic effects[1] and their potential application to non-linear optics.[2,3] These compounds have been used in the spectrophotometric determination of water in organic solvents[4,5] and for establishing a quantitative solvent polarity scale[1] to quantify the solvent effects on equilibrium constants and reaction rates.[6] Since the early detailed solvatochromic study performed by Reichardt and Dimroth,[7,8] pyridinium *N*-phenoxide betaine dyes (Fig. 1) have been extensively investigated for these purposes.

These dyes present a zwitterion-like structure in the electronic ground state, with positive and negative partial charges on the nitrogen and the oxygen atoms, respectively. This charge separation leads to very large ground-state dipole moments, which decrease significantly upon electronic excitation due to an intramolecular charge transfer (CT) from the phenoxide donor ring to the pyridinium acceptor fragment. Aryl substituents at the donor and/or the acceptor moieties modulate this transfer, shifting the CT absorption bands to either longer or shorter wavelengths. The most famous dye of this class of compounds is the zwitterion $E_T(30)$ Reichardt betaine, which has one of the largest measured solvatochromic shifts, ranging from a maximum at 453 nm in water to 810 nm in diphenyl ether, that is, a solvatochromic shift of 357 nm (9730 cm^{-1}).

The donor ring may be directly attached to the pyridinium nitrogen or to the carbon atoms of the pyridinium ring at the *meta* position. The betainic character, that is, the charge separation, is usually lost in the excited states with a charge transfer character, and in this case, the dipole moment in the ground state (μ_g) is much larger than that in the excited state (μ_e).

Alkyl and aryl substituted pyridinium *N*-phenoxide betaines have been studied experimentally by several research groups. Paley *et al.*[9] investigated the solvatochromic behavior of an *ortho*-betaine, 2,4-dimethyl-6-(2,4,6-triphenyl-*N*-pyridinio)-phenolate, for which they also obtained the crystallographic structure. The solvatochromic behavior of 2- and 4-pyridinio-phenoxides (Fig. 1a and 1b, respectively) has also been studied in a series of solvents.[10] In addition, semi-empirical (AM1), *ab initio* (HF/6-311G) and DFT (B3LYP/6-311G) methods have been employed[10] with the self-consistent reaction-field (SCRF) approach to rationalize these experimental data.

Several other theoretical treatments have been used to describe these betainic systems and their solvatochromic behavior, such as the single configuration interaction (CIS) study of the *para*-pyridiniophenoxide (Fig. 1b), where gas phase DFT molecular structures have been used to take into account the effects of the internal rotation on the calculated spectra in solution.[11] In fact, this molecular relaxation (internal rotation) appears to be quite important to understand the solvatochromic shifts. Also, Monte Carlo simulations of the $E_T(30)$ Reichardt betaine dye in twelve solvents have been performed aiming at understanding the molecular basis of the solvent polarity scale.[12] In that study,[12] *ab initio* (HF/6-31G*) and
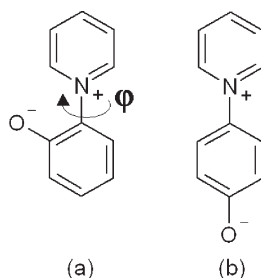

Fig. 1 (a) *ortho*- and (b) *para*-betaine.

semi-empirical (AM1 and INDO/S) methods have been used to determine the molecular structure and the charge distribution on the S_0 and S_1 states, in the gas phase. The solvent effects were derived from the electrostatic interactions between the effective charge distributions of the solvent molecules and the charge shift brought about by the $S_0 \rightarrow S_1$ transition. The dynamics of the $E_T(30)$ Reichardt betaine dye excited state has also been studied, in acetonitrile, using a hybrid classical/ quantum molecular dynamics method.[13] The π electrons of the solute have been treated quantum mechanically (PPP Hamiltonian), including the solvent influence on electronic structure, while the remaining interactions are treated *via* empirical potentials. As a result, the internal rotations were taken into account[13–16] but no attempt was made to explain the solvatochromic behavior of this system.

The main concern of the present work is then the calculation of the solvatochromism of one betaine taking into account the internal rotation between the phenoxide and the pyridinium rings. To accomplish this theoretical study we have chosen the *ortho*-betaine isomer (Fig. 1a) since it contains the basic donor–acceptor moieties of more complex betaines, such as the $E_T(30)$ Reichardt dye. Also, the *ortho*-betaine is small enough to be treated by *ab initio* methods and the effects of bulky groups are absent, so that the importance of the internal rotation or molecular relaxation in solution can be unambiguously ascertained. In addition, there is significant spectroscopic information about the solvatochromic behavior of this *ortho*-betaine in several solvents.[10] After choosing the appropriate betaine, a sequential hybrid quantum mechanical/Monte Carlo methodology[17–20] has been selected to study the solvatochromism and the effects of the molecular relaxation (internal rotation) in solution. More specifically, the Monte Carlo method has been used to yield statistically significant configurations of the solute–solvent system that were then treated by quantum chemical methods to obtain spectroscopic information. The combination of these methods in a sequential fashion should provide reliable theoretical results for a quantification of the effects of the internal rotation in the total solvent effects. As the solvent, we have chosen water as it gives the largest blue shift in the absorption spectrum where also the influence of hydrogen bonds can be studied.

Theoretical and computational procedures

The internal rotation or molecular relaxation is described by the dihedral angle between the phenoxide and the pyridinium rings, labeled φ, as shown in Fig. 1a. The *ab initio* MP2/6-31G method implemented in the Gaussian98 program[21] has been used to calculate the electronic and molecular structures and the electrostatic potential (EPS) fitted atomic charges[22] of the *ortho*-betaine at thirteen points on the reaction coordinate (φ) from $0°$ to $90°$ with a $7.5°$ step. Those 13 molecular structures were later used in the molecular simulations with rigid geometries and its respective atomic charges. In Fig. 2, the calculated charges of the oxygen and the nitrogen atoms and the dipole moment of the *ortho*-betaine are shown.

The interaction between the solute (*ortho*-betaine) and the solvent (water) is represented by a Lennard-Jones plus a Coulomb pair-wise potential. The SPC[23] parameters were used for the water molecules and the ESP fitted charges for the Coulombic part of the solute potential (see Fig. 2). The Lennard-Jones parameters (ε, σ) for the *ortho*-betaine were obtained from the phenol[24] and the pyridine[25] molecules. The standard geometric combination rules[26] were used to generate the pair-wise parameters. After defining the interaction potential, the Monte Carlo (MC) simulations were performed using standard procedures[26] for the Metropolis sampling technique in the canonical (NVT) ensemble, with periodic boundary conditions, image method and long range correction for the energy beyond the cut-off radius. The Lennard-Jones potential
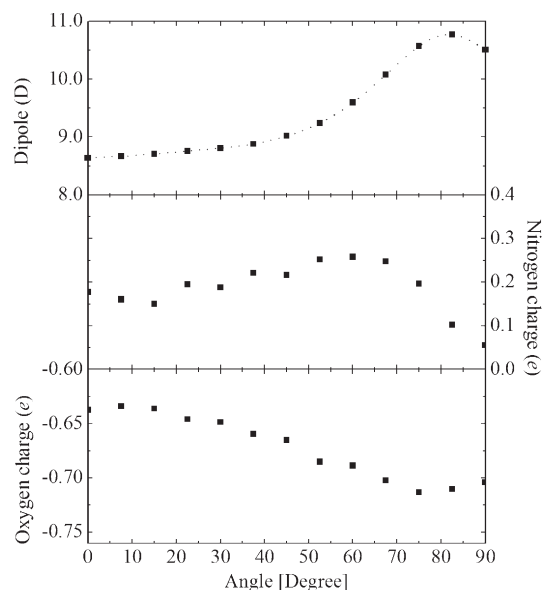
Fig. 2 The dipole moment and the atomic charges of the nitrogen and oxygen atoms as a function of the torsion angle obtained from electrostatic potential with MP2/6-31G. The dipole is shown in Debye and the charges in elementary charge unit.

contribution is estimated assuming a uniform distribution $G(r) \approx 1$ after the cutoff radius and the electrostatic potential contribution is estimated with the reaction field method of the dipolar interaction. The cut-off radius was considered as half-size of the cubic box length. The system was formed by one of the 13 molecular structures of the *ortho*-betaine surrounded by $N = 900$ water molecules. The experimental value for water density ($\rho = 0.9966$ g cm^{-3}) at $25°C$ was used to determine the size of the cubic box ($L = 3.011$ nm). The initial configurations were generated randomly and a new MC configuration was generated after N MC steps, *i.e.* after N molecules have been randomly selected and attempted to move.

The MC simulations were performed with DICE[27] and involved a thermalization stage of 9×10^6 MC steps followed by an average stage of 72×10^6 MC steps. In this averaging stage several thermodynamic and structural properties are calculated. Of special interest are the radial distribution functions and the variation of the Helmholtz energy due to the relative conformational stabilization of the *ortho*-betaine in aqueous solvation. The relative Helmholtz energy, $\Delta A(\varphi_i - \varphi_j)$, calculation is implemented in the MC simulation using the thermodynamic perturbation theory (TPT),[28–31] and was evaluated with a series of 6 separate simulations with the *ortho*-betaine in the rigid geometry but varying the torsion angle. We used the double-wide sampling,[25] *i.e.*, 6 simulations yielded 12 incremental free energy changes by perturbing the torsion angle φ_i to both sides: the smaller $\varphi_j = \varphi_i - 7.5°$ and the larger $\varphi_j = \varphi_i + 7.5°$, in each simulation. Consistent results have been obtained with TPT in various chemical and biochemical studies.[29–31]

Instead of performing a quantum mechanical calculation on every configuration generated by each simulation, we used the auto-correlation function or statistical efficiency, to select the statistically relevant configurations. In doing so, the subsequent quantum mechanical calculations were performed only on some uncorrelated structures. As in previous works,[17–20,32–35] we fitted the auto-correlation function of the energy to an exponentially decaying function and evaluated the correlation step. For the *ortho*-betaine in water, we obtained that configurations separated by an interval of 1.18×10^6 MC steps have less than 3% of statistical correlation. This assures that the configurations used in the quantum mechanical calculations are statistically uncorrelated and yield the same average values as the entire set of configurations.[34,35] Therefore, for each

simulation, we selected configurations separated by 1.18×10^6 successive configurations, generating a total of 61 statistically uncorrelated configurations, in which the quantum mechanical calculations were evaluated and averaged out.

The excitation energies were calculated using the Florida INDO program[36,37] within the INDO/CIS model[36] for the supermolecules generated by the MC simulation. The QM calculations were then performed for the supermolecular cluster composed of one *ortho*-betaine and all water molecules within a particular solvation shell. Each water molecule includes 8 valence electrons, and the Hartree–Fock wave function is anti-symmetric with respect to the entire solute–solvent system. CIS calculations were performed to obtain the excitation energies for all statistical uncorrelated configurations. The solvatochromic shift is obtained as the average over the 61 configurations used.

We identify the hydrogen bond (HB) structure around the oxygen atom of the betaine molecule, using both a geometric and energetic criteria.[18,33,38] Secondly, using the radial distribution function, we identify the first and second hydration shells. About 300 QM calculations of such clusters were performed in total. The largest cluster, involves the *ortho*-betaine and 150 solvent water molecules, including as much as 1264 valence electrons, properly anti-symmetrized in the self-consistent-procedure.

Results and discussion

The solvent effects on the conformation of the *ortho*-betaine have been calculated with the free-energy perturbation theory. These effects can be visualized by comparing the gas phase internal rotation energy (MP2/6-31G) and the Helmholtz energy internal rotation (TPT-MC) as shown in Fig. 3. There are significant qualitative as well as quantitative differences between the internal rotation in the gas phase and in water. The most stable conformer is shifted from approximately 30° in the gas phase to near 60° in water. Also, the maximum in the potential energy corresponds to 90° in the gas phase whereas in water it is shifted to 0°. The minimum of the Helmholtz energy profile in water is very flat compared to the potential energy minimum in the gas phase. The barrier to internal rotation changes from approximately 7 kcal mol^{-1} in the gas phase to around 5 kcal mol^{-1} in water. At this stage an important point is whether the solute electron distribution polarized by the solvent will significantly change the result for the
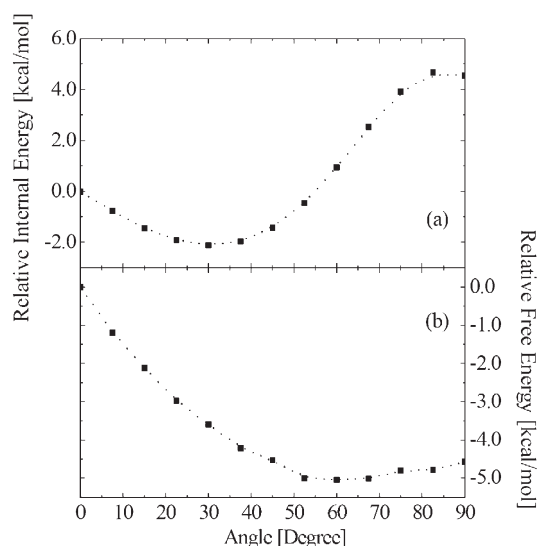
torsion angle. Additional calculation made using the PCM[39] method showed that a similar pattern arises. The solvent changes the equilibrium angle of the gas phase from 30° to a value of ∼70° with an energy surface that is very flat, similar to the result obtained for the Helmoltz free energy discussed above.

These results are significant since it is common practice to just include the solvent effects into the gas phase potential energy surface or even use only the most stable conformer in the gas phase for simulations in solutions. This twist angle has been noted in the $E_T(30)$ Reichardt betaine.[12,15,16] In the present case it is clear that there is a soft inter-ring rotation mode associated with the flat potential of *ortho*-betaine in water.

The radial distribution function, RDF, for the most stable conformer in solution ($\varphi = 60°$), is shown in Fig. 4. Fig. 4a shows the RDF between the oxygen atom of the *ortho*-betaine and the hydrogen atoms of the water, Fig. 4b shows the RDF between the oxygen atom of the *ortho*-betaine and the oxygen atom of the water and Fig. 4c shows the RDF of the closest atoms between the solute and solvent molecules. This is a nearest-neighbor[40] RDF that is more appropriate in defining the solvation shell for betaine. It is of interest to analyze separately the contribution of the hydrogen bonds. The criteria utilized to classify a hydrogen bond was composed of a geometrical (radial distance $R_{O\cdots O} \leq 3.35$ Å and angular $O\hat{O}H \leq 30.0°$) and an energetic (binding $E_{HB} \geq 3.6$ kcal mol^{-1}) contribution. The adequacy of this procedure has been discussed elsewhere.[38] We find that in 8.2% of the configurations the phenoxyde oxygen makes one hydrogen bond with water molecules, in 54.1% of the configurations it makes two hydrogen bonds and in 37.7% it makes three hydrogen bonds. In total, we find that there is an average of 2.3 hydrogen bonds for the phenoxyde oxygen atom (proton acceptor). This is termed as the HB shell. Fig. 4c shows additional hydration shells for the *ortho*-betaine at this conformation. As it can be seen there is a clear nearest-neighbor solvation shell that starts at 1.5 Å and ends at 4.0 Å, that gives a total of 30 water molecules. After this, only a broad feature is observed, but it is still possible to note some structure that ends at around 7.45 Å, that gives a total of 50 water molecules. To have a larger cluster for the quantum mechanical calculations we use the hydration shell distances of 9.65 Å yielding 120 water molecules

Fig. 3 Relative internal energy and Helmholtz energy as a function of the torsion angle obtained with *ab initio* calculations with MP2/6-31G and with TPT in the MC simulation, respectively.
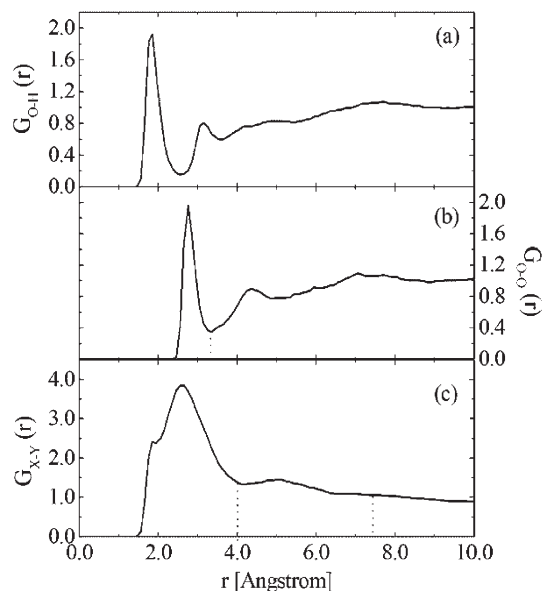
Fig. 4 Radial distribution function between (a) the oxygen of *ortho*-betaine and the hydrogen atom of water, (b) the oxygen of *ortho*-betaine and the oxygen atom of water and (c) between all atoms of the *ortho*-betaine and the nearest atom of each water molecule.

around the *ortho*-betaine and of 10.40 Å yielding 150 water molecules. Table 1 specifies the hydration shells that are used in the quantum mechanical calculations of the electronic spectrum. Note that in the HB shell, in the total of 61 configurations used in the quantum calculations, 5 have only one water molecule bonded in the *ortho*-betaine, 33 have two water molecules and 23 have three, giving a total of 72, 82 and 88 valence electrons, respectively.

The selected configurations have been submitted to quantum chemical calculation with the INDO/CIS model to obtain the solvent effects in the transition energies. Quantum mechanical calculations are made with several cluster sizes to analyze the influence of the outer solvation shells in the solvatochromic shift. The bulk result can then be obtained[18,33] extrapolating the calculating transition energy shifts for different solvation distances, as shown in Fig. 5. The results for the individual contributions of each hydration shell, including the bulk limit, to the solvatochromism of the *ortho*-betaine are summarized in Table 2. We first analyze the influence of the torsion angle on the gas phase spectrum. Changing the angle from 30° to 60° yields significant shifts. The first $\pi \rightarrow \pi^*$ transition is red shifted by nearly 2000 cm^{-1}, whereas the first $n \rightarrow \pi^*$ transition suffers a blue shift of 1600 cm^{-1}. In Fig. 6, the filled circles show the effect in the first $n \rightarrow \pi^*$ transition due to the changing in the torsion angle relatively to the transition value in the 30°. As can be seen for torsion angles smaller than 30° the transition energy is red shifted, reaching -3167 cm^{-1} in the planar conformation (*i.e.* $\varphi = 0°$). Whereas for torsion angles larger than 30° the transition is blue shifted, reaching 1682 and 1607 cm^{-1} for conformations with $\varphi = 50°$ and 60°. This curve shows that conformational changes in the *ortho*-betaine can induce a shift of around 4800 cm^{-1} in the first $n \rightarrow \pi^*$ transition.

The influence of the solvent is given in the lower part of Table 2. Adding the HB shell yields pronounced shifts for all absorption bands considered here. However, these are still very small compared to the total shifts. The $n \rightarrow \pi^*$ transition suffers a blue shift of 3136 cm^{-1} due to the HB shell, which can be separated into 1529 cm^{-1} due to the electronic contribution and 1607 cm^{-1} due to the solute relaxation. Table 2 also gives the separate contribution of the hydration shell to the total calculated solvatochromic shifts.

The final calculated solvatochromic value of 6060 ± 89 cm^{-1} for the $n \rightarrow \pi^*$ transition is in reasonable agreement with the observed value of 7552 cm^{-1}, obtained as the shift of the maximum in the absorption spectra of the *ortho*-betaine in water and toluene.[10] The difference is probably due to inherent deficiencies of the INDO/CIS method as well as due to the effects of other conformations near 60°, since the Helmholtz energy is somewhat flat around the minimum. The difference is also due to the comparison between the gas phase/water with the toluene/water shifts. It can be seen that changing the dihedral angle from 30° to 60° causes, in the gas phase, a red shift of all $\pi \rightarrow \pi^*$ transitions, which can be as large as 1986 cm^{-1}, and a blue shift of 1607 cm^{-1} for the $n \rightarrow \pi^*$ transition. These results show the importance of the molecular relaxation for the absorption spectrum. Regarding the solvent effects, Table 2 presents the solvatochromism of the most stable conformer

in water ($\varphi = 60°$) with respect to the most stable conformer in the gas phase ($\varphi = 30°$).

It is worthwhile noticing that the solvent causes a blue shift for the $\pi \rightarrow \pi^*$ transition. In fact, these data contain both the molecular relaxation and the solvent effects. Assuming that these effects are additive, the shift due to only the solvent effects can be estimated by subtracting off the molecular relaxation shift obtained from the gas phase calculation. This procedure yields the "net solvent effects" on the solvatochromism, which are listed in the last row of Table 2. In Fig. 6, the open circles show the effect of the 120 water molecules in the first $n \rightarrow \pi^*$ transition relatively to the transition value of the isolated *ortho*-betaine in the 30° conformation. The net solvent effect is the difference between the filled and the open circles for each torsion angle. The smallest effects, around 1000 cm^{-1}, can be seen for torsion angles smaller than 40° and the largest effects, around 4500 cm^{-1}, can be seen for torsion angles larger than 70°. Depending on the conformation of the *ortho*-betaine the net solvent effect can vary from 934 to 4636 cm^{-1} and therefore the net solvent effects can be larger or smaller than the molecular relaxation effects. Thus those two effects, solvent and geometry relaxation, are both very important for a qualitative and quantitative description of the solvatochromism. The solute relaxation is also important for understanding the solvent polarity scale associated with the solvatochromic shifts of the $E_T(30)$ Reichardt dye.[14,15,41]
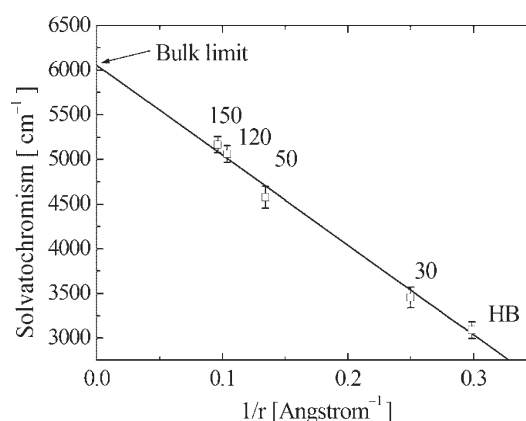

Fig. 5 Extrapolation of the calculated $n \rightarrow \pi^*$ transition energy to the bulk limit. HB, first, second and others hydration shells are shown.

Table 1 Properties of the hydration shells

	HB	First	Second	Others	
Number of water molecules in the shell	~2.3	30	50	120	150
Number of valence electrons for each shell	~82	304	464	1024	1264
Average distance hydration shell–solute/Å	3.35	4.00	7.45	9.65	10.40

Table 2 Transition energies (in cm^{-1}) and solvatochromic shift (in cm^{-1}) for the *ortho*-betaine in the gas phase ($\varphi = 30°$) and aqueous solution ($\varphi = 60°$)

	Transition	
Gas phase	$\pi \rightarrow \pi^*$	$n \rightarrow \pi^*$
Transition energy (φ_{30})	15 612	22 798
Transition energy (φ_{60})	13 626	24 405
ΔE ($\varphi_{60} - \varphi_{30}$)	-1986	1607

ΔE = transition energy at 60° − transition energy at 30°

$\langle \Delta E([\varphi_{60} + \text{HB}] - \varphi_{30}) \rangle^a$	-1234 ± 40	3136 ± 69
$\langle \Delta E([\varphi_{60} + 30\text{H}_2\text{O}] - \varphi_{30}) \rangle$	-162 ± 107	3456 ± 114
$\langle \Delta E([\varphi_{60} + 50\text{H}_2\text{O}] - \varphi_{30}) \rangle$	36 ± 111	4578 ± 120
$\langle \Delta E([\varphi_{60} + 120\text{H}_2\text{O}] - \varphi_{30}) \rangle$	389 ± 98	4955 ± 94
$\langle \Delta E([\varphi_{60} + 150\text{H}_2\text{O}] - \varphi_{30}) \rangle$	483 ± 80	5230 ± 85
$\langle \Delta E([\varphi_{60} \text{ bulk limit}] - \varphi_{30}) \rangle^b$	1026 ± 69	6060 ± 89
Net solvent effects	3012 ± 69	4453 ± 89

[a] The error is associated with the standard deviation of the 61 configurations used. [b] The estimate value and the error is related to the linear regression fitting as can be seen in Fig. 5.
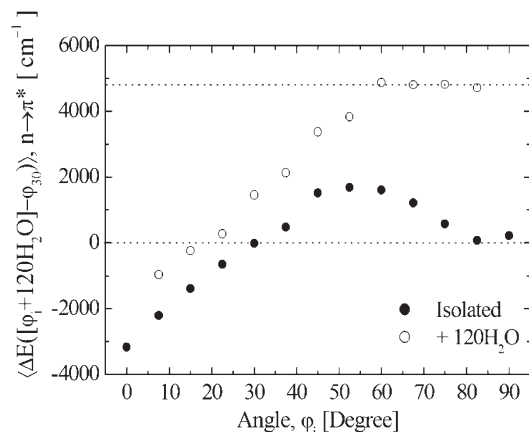
Fig. 6 The calculated n → π* transition energy (in cm⁻¹) with respect to the conformation with φ = 30° as a function of the torsion angle. The filled circles are the results obtained for the isolated *ortho*-betaine and the open circles are the averaged results obtained for 61 configurations of one *ortho*-betaine surrounded by 120 water molecules.

In the case of the most stable conformer in water ($\varphi = 60°$) shown in Table 2, the internal rotation relaxation amounts to nearly 30% of the total computed shift. It should also be emphasized that the simulation of the solvent by only including hydrogen bonded molecules is inadequate even for a qualitative description. Indeed the blue shift of the $\pi \rightarrow \pi^*$ transitions are not obtained if only the HB shell is considered. In fact, cluster calculations need to consider at least 50 solvent molecules to yield a qualitative result, and nearly 150 molecules for a reasonable quantitative description. The necessity of including outer hydration shells extending far beyond the solute is likely to be a consequence of the large dipole moment of betaines.

Conclusions

It has been shown that the molecular relaxation due to the solvent effects on the conformation is quite important for a proper description of the solvatochromism of the flexible *ortho*-betaine. In fact, the molecular relaxation has an opposite effect on the solvatochromic shift for the $\pi \rightarrow \pi^*$ transitions when compared to the net solvent effects. These approximately separated contributions to the solvatochromism allowed the quantification of the molecular relaxation effects, which are significant for even a qualitative description.

Acknowledgements

References

1 C. Reichardt, *Solvent Effects in Organic Chemistry*, Verlag Chemie, Weinheim, New York, 1979.
2 M. S. S. Palay and J. M. Harris, *J. Org. Chem.*, 1991, **56**, 568.
3 J. Abe, N. Nemoto, Y. Nagase and Y. Shirai, *Chem. Phys. Lett.*, 1996, **261**, 18.
4 S. Kumoi, K. Ogyama, H. Yano, H. Kobayashi and K. Ueno, *Talanta*, 1970, **17**, 319.
5 H. Langhals, E. Fritz and I. Mergelsberg, *Chem. Ber.*, 1980, **1980**, 3662.
6 M. J. Kamlet, J. L. M. Abboud and W. R. Taft, *Prog. Phys. Org. Chem.*, 1981, **13**, 485.
7 K. Dimroth, C. Reichardt, T. Siepmann and F. Bohlmann, *Justus Liebigs Ann. Chem.*, 1963, **661**, 1.
8 C. Reichardt, *Angew. Chem., Int. Ed. Engl.*, 1965, **4**, 29.
9 M. S. Paley, E. J. Meehan, C. D. Smith, F. E. Rosenberger, S. C. Howard and J. M. Harris, *J. Am. Chem. Soc.*, 1989, **54**, 3432.
10 D. González, O. Neilands and M. C. Rezende, *J. Chem. Soc., Perkin Trans.*, 1999, **2**, 713.
11 J. Fabian, G. A. Rosquete and L. A. Montero-Cabrera, *J. Mol. Struct. (THEOCHEM)*, 1999, **469**, 163.
12 S. R. Mente and M. Maroncelli, *J. Phys. Chem. B*, 1999, **103**, 7704.
13 J. Lobaugh and P. J. Rossky, *J. Phys. Chem. A*, 1999, **103**, 9432.
14 T. Ishida and P. J. Rossky, *J. Phys. Chem. A*, 2001, **105**, 558.
15 J. Lobaugh and P. Rossky, *J. Phys. Chem. A*, 2000, **104**, 899.
16 W. Bartkowiak and J. Lipinski, *J. Phys. Chem. A*, 1998, **102**, 5236.
17 K. Coutinho and S. Canuto, *Adv. Quantum Chem.*, 1997, **28**, 89.
18 S. Canuto and K. Coutinho, *Int. J. Quantum Chem.*, 2000, **77**, 192.
19 K. Coutinho, S. Canuto and M. C. Zerner, *J. Chem. Phys.*, 2000, **112**, 9874.
20 K. J. Almeida, K. Coutinho, W. B. De Almeida, W. R. Rocha and S. Canuto, *Phys. Chem. Chem. Phys.*, 2001, **3**, 1583.
21 M. J. Frisch, G. W. Trucks, H. B. Schlegel, G. E. Scuseria, M. A. Robb, J. R. Cheeseman, V. G. Zakrzewski, J. A. Montgomery Jr., R. E. Stratmann, J. C. Burant, S. Dapprich, J. M. Millam, A. D. Daniels, K. N. Kudin, M. C. Strain, O. Farkas, J. Tomasi, V. Barone, M. Cossi, R. Cammi, B. Mennucci, C. Pomelli, C. Adamo, S. Clifford, J. Ochterski, G. A. Petersson, P. Y. Ayala, Q. Cui, K. Morokuma, D. K. Malick, A. D. Rabuck, K. Raghavachari, J. B. Foresman, J. Cioslowski, J. V. Ortiz, A. G. Baboul, B. B. Stefanov, G. Liu, A. Liashenko, P. Piskorz, I. Komaromi, R. Gomperts, R. L. Martin, D. J. Fox, T. Keith, M. A. Al-Laham, C. Y. Peng, A. Nanayakkara, C. Gonzalez, M. Challacombe, P. M. W. Gill, B. Johnson, W. Chen, M. W. Wong, J. L. Andres, C. Gonzalez, M. Head-Gordon, E. S. Replogle and J. A. Pople, GAUSSIAN 98, Revision A.7, Gaussian, Inc., Pittsburgh PA, 1998.
22 C. M. Breneman and K. B. Wiberg, *J. Comput. Chem.*, 1990, **11**, 361.
23 H. J. C. Berendsen, J. P. M. Postma, W. F. van Gunsteren and J. Hermans, *Intermolecular Forces*, ed. B. Pullmam, Reidel, Dordrecht, 1981.
24 W. L. Jorgensen and T. B. Nguyen, *J. Comput. Chem.*, 1993, **14**, 195.
25 W. L. Jorgensen, J. M. Briggs and M. L. Contreras, *J. Phys. Chem.*, 1990, **94**, 1683.
26 M. P. Allen and D. J. Tildesley, *Computer Simulation of Liquids*, Clarendon Press, 1987.
27 K. Coutinho and S. Canuto, *DICE: A Monte Carlo program for molecular liquid simulation*, University of São Paulo, 1997.
28 R. W. Zwanzig, *J. Chem. Phys.*, 1954, **22**, 1420.
29 C. A. Reynolds, P. M. King and W. G. Richards, *Mol. Phys.*, 1992, **76**, 251.
30 T. P. Straatsman and J. A. McCammon, *Annu. Rev. Phys. Chem.*, 1992, **43**, 407.
31 P. Kollman, *Chem. Rev.*, 1993, **93**, 2395.
32 K. Coutinho, S. Canuto and M. C. Zerner, *Int. J. Quantum Chem.*, 1997, **65**, 885.
33 K. Coutinho and S. Canuto, *J. Chem. Phys.*, 2000, **113**, 9132.
34 K. Coutinho, M. J. De Oliveira and S. Canuto, *Int. J. Quantum Chem.*, 1998, **66**, 249.
35 W. R. Rocha, K. Coutinho, W. B. De Almeida and S. Canuto, *Chem. Phys. Lett.*, 2001, **335**, 127.
36 J. Ridley and M. C. Zerner, *Theor. Chim. Acta*, 1973, **32**, 111.
37 M. C. Zerner, INDO: A semi-empirical program package, University of Florida, Gainesville, FL 32 611 1973.
38 E. E. Fileti, K. Coutinho, T. Malaspina and S. Canuto, *Phys. Rev. E*, 2003, **67**, 61 504.
39 S. Miertus, E. Scrocco and J. Tomasi, *Chem. Phys.*, 1981, **55**, 117.
40 K. Coutinho and S. Canuto, *Adv. Quantum Chem.*, 2002, **41**, 161.
41 V. Znamenskiy and M. N. Kobrak, *J. Phys. Chem. B*, 2004, **108**, 1072.